

Excitonic absorption edge of indium selenide

J. Camassel, P. Merle, and H. Mathieu

Centre d'Etudes d'Electronique des Solides, Université des Sciences et Techniques du Languedoc, 34060-Montpellier Cedex, France*

A. Chevy

Laboratoire de Luminescence, Université Pierre et Marie Curie, 75230-Paris Cedex-05, France*

(Received 19 December 1977)

We report an investigation of the fundamental absorption edge of InSe under high-resolution conditions. We resolve three components of the direct exciton series and obtain an effective Rydberg energy of 14.5 meV. From this value an effective mass ($m = 0.10 m_0$) of electrons in the Γ minimum of the conduction band is obtained. We analyze the absorption coefficient with a three-dimensional model and find a remarkable agreement. We deduce an interband matrix element in polarization $\vec{E} \perp \vec{C}$: $P_{\perp}^2 = 0.6$ eV. Next we investigate the temperature dependence of the fundamental absorption edge. We find a strong interaction with a 14-meV phonon which accounts for (i) the shift of the band-gap energy in the full temperature range between liquid-helium temperature and 300°K and (ii) the temperature dependence of the broadening parameter (exciton lifetime). A simple analytical expression is obtained which accounts for the temperature dependence of the band gap and the $n = 1$ exciton structure. Last, we deduce the electron-phonon coupling constant.

I. INTRODUCTION

The near-band-edge optical and electrical properties of strongly anisotropic crystals are a subject of considerable technical interest. In the recent years, among the III-VI layer crystals, GaSe has been the most investigated¹ and the three-dimensional character of the charge carriers in this compound now appears to be well established.² However, it is not clear whether the small anisotropy reported in GaSe is a specific feature of this crystal or a general property of all III-VI layer compounds. In order to clarify this point, we have investigated the closely related compound InSe. The basic layer structure is similar to GaSe. It is made of a fourfold stacking of selenium-indium-indium and selenium-atom sheets which characterizes all M_2X_2 molecularlike crystals (see Fig. 1). The Bridgman grown crystals usually belong to the γ modification³; their unit cell is rhombohedral and extends over three layers. It contains three M_2X_2 molecular units.

Until now, only the optical properties at the fundamental absorption edge,⁴ the reflectivity spectrum up to 12 eV,⁵ and the UPS and XPS (ultraviolet and x-ray photoemission) valence-band-density-of-states spectra⁶ have been reported. All sets of data are restricted to temperatures in the range 90–293 °K and show strong similarities with GaSe. An indirect absorption edge E_{gi} , at 1.285 eV at 90 °K with a temperature coefficient $dE_{gi}/dT = -4.2 \times 10^{-4}$ eV/°K, was reported and a phonon of energy 21 ± 5 meV was found to assist the transition. More recently, photovoltaic measurements⁷ have confirmed this interpretation.

The next threshold is a direct transition with a strong excitonic character. The position of the $n = 1$ structure was reported at 1.320 eV (90 °K) and the corresponding exciton binding energy R_0 was 37 meV, almost twice the value reported for GaSe.⁸ The series of interband energies⁵ obtained in reflectivity closely parallel the results for GaSe and, finally, a recent semiempirical band-structure calculation⁹ together with the photoemission spectra⁶ confirms this overall similitude.

In this paper, we report new data obtained at pumped liquid-helium temperature in the fundamental absorption region. For the first time, we have resolved the three components corresponding to the ground state ($n = 1$) and two excited states ($n = 2, n = 3$) of the direct exciton series. We report a new and reliable value of 14.5 ± 0.5 meV for the binding energy. We have used this value to fit the absorption spectrum with the three-dimensional exciton theory¹⁰ assuming a Lorentzian broadening.¹¹ We get a satisfactory agreement and obtain the transition-matrix element in polarization $\vec{E} \perp \vec{C}$. We find $P_{\perp}^2 = 0.6$ eV which constitutes the first estimate of an interband matrix element for a III-VI layer compound.

Next we have investigated the temperature dependence of the band gap from 1.6 to 300 °K. It has been shown in GaSe that most of the strength of the electron-phonon interaction concentrates on a 16.5-meV phonon mode which accounts well for the temperature dependence of the band gap in the range 4.2–300 °K (self-energy effect).¹² We find similar results for InSe with a 14-meV phonon. This energy is in good agreement with the results of a simple mass scaling between

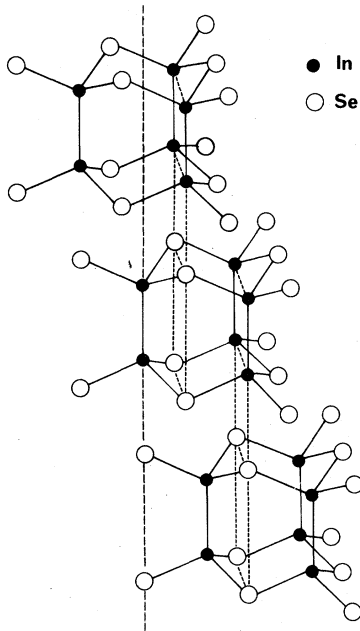


FIG. 1. Perspective view of a γ polytype for InSe (space group symmetry C_{3v}^2). The unit cell extends over three layers. Within a layer one recognizes the pyramidal p^3 coordination of selenium atoms (outermost atoms) and the tetrahedral sp^3 coordination of indium atoms in the two central sheets. Note the close packing of selenium p^3 pyramids within two neighboring layers. Note also the successive repetition of two selenium atoms, two gallium atoms, and one empty space along the vertical lines drawn in the figure. These lines extend over the unit cell.

GaSe and InSe. Finally, we find that the same electron-phonon interaction rules the temperature dependence of the broadening parameter in the full temperature range. Within the three-dimensional limit, we compare the experimental change with a theoretical model and obtain the electron-phonon coupling constant.

The arrangement of the paper is the following. First, we discuss the details of the experimental procedure. Second, we briefly set the theoretical background needed for the analysis of our data, and we compare our experimental results with GaSe. Third, we discuss the temperature dependence of the band-gap and the electron-phonon interaction.

II. EXPERIMENTAL DETAILS AND TYPICAL RESULTS

Thin samples about $10 \mu\text{m}$ thick were cleaved from a large single crystal of InSe grown by a nonstoichiometric Bridgman method from an $\text{In}_{1.12}\text{Se}_{0.88}$ melt. The resulting crystals have stoichiometric compositions.¹³ They are N type,

with about 10^{15} carriers/ cm^3 and $500 \text{ cm}^2/\text{V sec}$ mobility. They cleave very easily and permit us to get thin mirrorlike samples perpendicular to the C axis. For the very low temperature experiments, they are mounted in a strain-free manner inside a liquid-helium bath pumped below the λ point. In the intermediate range of temperature an exchange gas technique is used.

Our experimental setup has been already described.¹⁴ In this work, we have used our high-resolution THR 1500 Jobin-Yvon spectrometer with a 1200 grooves/mm holographic grating in first-order and single pass configuration. This allows a practical resolution of $1/30\,000$. The detector was a silicon photodiode with the light beam intensity chopped at about 300 Hz. Standard lock-in amplification techniques were used.

In all experiments, the energy dependence of the transmitted light was carefully checked below the threshold. It closely followed the energy dependence of the incident intensity I_0 , but exhibited strong multiple internal reflection effects. The sample thickness was calculated from these interference patterns assuming $n=3$,¹⁵ and a negligible dispersion of the ordinary refractive index. In all cases, the absorption coefficient values were obtained from the transmitted intensity assuming $\alpha=0$ in the range of constant I_T/I_0 . Last, the light beam propagation direction was kept parallel to the

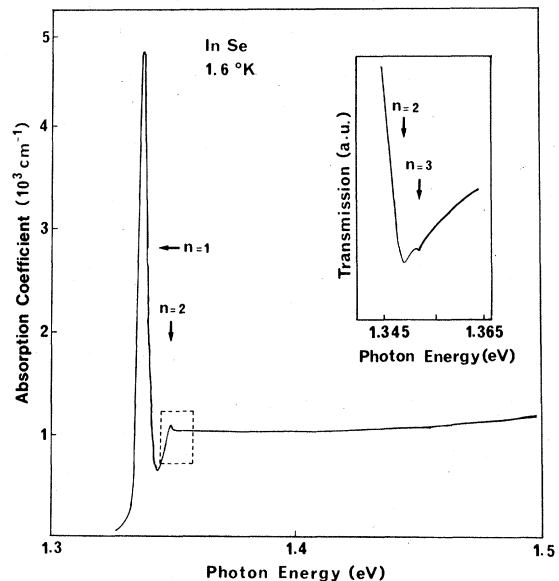


FIG. 2. Experimental absorption spectrum obtained at low temperature on a $7\text{-}\mu\text{m}$ -thick InSe sample. The insert displays on an expanded scale an experimental transmission spectrum. It shows, clearly resolved, the $n=2$ and $n=3$ excitonic structures discussed in the text. The resolution is 0.05 meV .

C axis which corresponds to the standard $\vec{E} \perp \vec{C}$ configuration and no attempt was made in this work to investigate the interband matrix element parallel to \vec{C} .

A typical spectrum obtained at 1.6°K on a 7- μ m-thick sample is shown in Fig. 2. We must remark the fairly high level of absorption reached on the first $n=1$ excitonic level ($\alpha \sim 5000 \text{ cm}^{-1}$) and the resolution of the two excited states $n=2$ and $n=3$. This is better shown in the insert which displays on an expanded scale an experimental transmission spectrum. Note the weakness of the structure associated with $n=3$ as compared with the first excited state ($n=2$). Also note the fairly constant "plateau" reached above the band gap. We have not been able to resolve the indirect gap structure reported in Refs. 4 and 7 and we shall discuss in this work only the lowest direct excitonic transition around 1.338 eV.

III. THEORETICAL BACKGROUND AND ANALYSIS OF THE LOW-TEMPERATURE DATA

The layer structure of InSe corresponds with the γ polytype of GaSe (rhombohedral modification).^{3,13} The space group symmetry is C_{3v}^5 and the unit cell which extends over three layers contains three $M_2 X_2$ units (see Fig. 1). Within a layer one recognizes the fourfold stacking of monoatomic sheets which characterizes the pyramidal p^3 coordination of selenium (outermost atoms). Each selenium atom is bound with three tetrahedrally coordinated metal atoms which lie in the two central sheets. The saturation of Se p -like orbitals determines most of the physical properties of the crystals. It leaves two unpaired electrons on two neighboring In atoms which couple to form the In-In covalent bond directed along the C axis. This bond plays an important part in the description of electronic levels near the band gap.

From the viewpoint of band-structure calculations, we expect many results from β polytype of GaSe (Refs. 16 and 17) to be directly extended to γ -InSe. Indeed it has been shown both experimentally¹⁸ and theoretically¹⁹ that the effect of polytypism on the electronic energy position of band-gap levels for GaSe never exceeds 5 to 50 meV. The main difference between GaSe and InSe arises from their different metal-metal bond length: GaSe has a shorter bond length, thus a stronger coupling and a larger band gap. Anyway we expect^{9,16,17} the topmost valence band to have a Γ_1 symmetry (see Table I) and to show a strong admixture of In-In bonding S states with Se p_x -like states. In the same ways we expect the lowest conduction band to have a Γ_2 symmetry and a strong indium-indium antibonding character. In the single group notation, the com-

TABLE I. Symmetries of the wave functions and dipole operator, in the single-group notation for (i) a single layer and/or an ϵ polytype (D_{3h}), (ii) a β polytype (D_{6h}) and (iii) a γ polytype (C_{3v}). The fundamental transition is forbidden in polarization $\vec{E} \perp \vec{C}$ for all three polytypes.

Symmetry	Polytype		
	β	ϵ	γ
Point group	D_{6h}	D_{3h}	C_{3v}
Conduction band	Γ_3^+	Γ_2	Γ_2
Valence band	Γ_4^-	Γ_1	Γ_1
Dipole operator			
P_{\parallel}	Γ_2^-	Γ_2	Γ_2
P_{\perp}	Γ_6^-	Γ_5	Γ_3

patibility relations for point group symmetries D_{6h} , D_{3h} , and C_{3v} are summarized in Table I. We find the symmetry of the dipole operator for light polarized $\vec{E} \perp \vec{C}$ to be Γ_3 : the fundamental transition $\Gamma_1 \rightarrow \Gamma_2$ is dipole forbidden for InSe. It becomes allowed through a weak spin-orbit interaction in the double group representation, but should have a relatively small oscillator strength. This is the case for GaSe for which the most recent report²⁰ gives $\alpha_{\text{max}} \sim 6000 \text{ cm}^{-1}$ at 2°K. In Fig. 2 we find for InSe a maximum absorption value around 5000 cm^{-1} , which confirms the GaSe-like scheme.⁹

From the energy position of the three excitonic transitions resolved in Fig. 2, we could deduce a value of the exciton binding energy in different ways. The results obtained at 1.6, 8, 11, and 20°K are summarized in Table II. A brief compilation gives, from the two first excitonic structures, a fairly constant value, $R_0 = 14.5 \pm 0.5 \text{ meV}$. The results obtained with the most excited state ($n=3$) appear less reliable.

TABLE II. Values of the binding energy (meV) obtained for the direct exciton of InSe at various temperatures and from different excitonic lines. The result ascertained by the theoretical fit is $R_0 = 14.5 \pm 0.5 \text{ meV}$.

T (°K)	1.6	8	11	20
$E_{n=1}$	1338.3	1337.9	1337.4	1336.8
$E_{n=2}$	1349.2	1348.8	1348.4	1348
$E_{n=3}$	1.352	1351.9	1351.6	1350.5
$R_0 = \frac{R}{6} (E_{n=3} - E_{n=1})$	15.4	15.7	16	15.4
$R_0 = \frac{R}{3} (E_{n=2} - E_{n=1})$	14.5	14.5	14.6	14.9

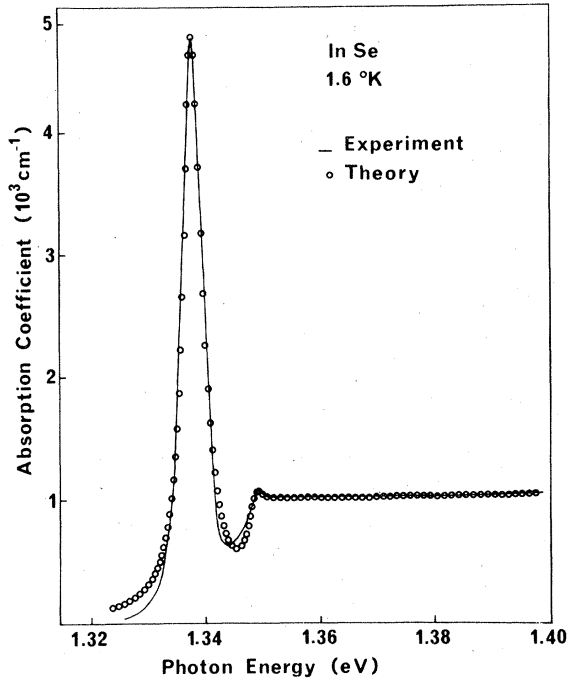


FIG. 3. Comparison of our experimental results with a three-dimensional model as explained in the text. No free parameters enter the calculation: the linewidth (2 meV) and effective Rydberg (1.45 meV) are obtained from experimental data, the normalization constant represents the absorption strength above the band gap and equals 1050 cm^{-1} . The agreement obtained is remarkable; it shows clearly the three-dimensional character of excitons in InSe.

In order to ascertain this result, we have attempted a fit in light of the three-dimensional theory of direct allowed excitonic transitions.¹⁰ However, the theoretical results ignore the experimental broadening effect. In order to get a more realistic picture, we have convoluted the theoretical expression for $\alpha(\hbar\omega)$ (Ref. 10) with a Lorentzian function $\Gamma\pi^{-1}(E^2 + \Gamma^2)^{-1}$ (Ref. 11), where Γ is the half width at half maximum of the Lorentzian and the associated lifetime is $\hbar/2\Gamma$. Until now this is the first attempt reported at very low temperature when both $n=1$ and $n=2$ levels are clearly resolved. We have used the standard convolution product^{11,21,22}

$$\alpha_c(\hbar\omega) = \frac{1}{(2\pi)^{1/2}} \int_{-\infty}^{\infty} \alpha(\hbar\omega - E) \frac{\Gamma}{\pi(E^2 + \Gamma^2)} dE, \quad (1)$$

where the unbroadened absorption coefficient¹⁰ is

$$\alpha(\hbar\omega) = A \left(\sum_{n=1}^{\infty} \frac{2R_0}{n^3} \delta(\hbar\omega - \hbar\omega_n) + \frac{U(\hbar\omega - E_g)}{1 - e^{-2\pi Z}} \right). \quad (2)$$

A is a normalization constant connected with the

effective masses μ , a dimensionless interband oscillator strength f_{cv} , and the refractive index n

$$A = \frac{(2\mu)^{3/2} e^2 f_{cv} 2\pi R_0^{1/2}}{nc\hbar^2 m_0}. \quad (3)$$

U is the unit step function, $Z = [R_0/(\hbar\omega - E_g)]^{1/2}$, and $f_{cv} = P_1^2/2E_g$.

With the fixed value $R_0 = 14.5$ meV and the experimental broadening parameter $\Gamma = 2$ meV, the only adjustable parameter is the normalization constant A , which represents the absorption strength at the band gap when $\Gamma = 0$. For a given compound it is a characteristic parameter, independent of the temperature, as are the Rydberg energy, effective masses, etc. We shall come back to that point in Sec. IV.

In Fig. 3, the best fit is obtained with $A = 1050 \text{ cm}^{-1}$ and the result is shown as open circles on the experimental data (full line). The general agreement is remarkable, except for a small discrepancy for the low values of α . It shows clearly the three-dimensional character of excitons in InSe. As the maximum value $\alpha_M \sim 4900 \text{ cm}^{-1}$ is well reproduced in the calculation, as well as the shape and magnitude of the $n=2$ excitonic structure, we think that the slight discrepancy found in Fig. 3 is due to an overestimate of the absorption feet introduced by the Lorentzian form in Eq. (1). The excitonic lifetime which is associated with the broadening parameter $\Gamma = 2$ meV, at 1.6°K , is about 10^{-12} sec.

From our binding energy $R_0 = 14.5$ meV, we can estimate the electronic effective mass in the Γ minimum of the conduction band. With $\epsilon_0 = 9$, we get $\mu = 0.09 m_0$ for the isotropic value of the exciton reduced mass. However, we lack information concerning the hole effective masses in InSe. We have taken an average value $m_n = 0.5m_0$ between all results reported for GaSe,^{2,8,12,23} and GaTe.²⁴ This gives for the electrons at $k=0$ an isotropic value $m_e = 0.10m_0$ which is two times smaller than the corresponding isotropic value reported for GaSe,^{2,8} but correlates well with the trend found in III-V compounds between GaSb and InSb.²⁵

The Bohr radius of excitons which is obtained from the reduced mass, $\mu = 0.09m_0$, is about 50 Å. This is fairly large and corresponds to a real-space extension over six monolayers or two unit cells of the γ polytype.^{3,9,13} This explains qualitatively the three-dimensional character found in Fig. 3.

Finally, we have estimated the transition matrix element connecting the valence and conduction bands in the $\vec{E} \perp \vec{C}$ configuration. From the best-fit value of $A = 1050 \text{ cm}^{-1}$, we got $P_1^2 = 0.6 \text{ eV}$, which is about twenty times lower than the typical value for a cubic compound.^{11,25} As far as we know, this

is the first estimate of an interband matrix element for a III-VI layer compound.

IV. TEMPERATURE DEPENDENCE OF THE BAND EDGE

A. Results

Our experimental results for the temperature dependence of the $1s$ excitonic structure in the range 1.6 – 300 °K are shown in Fig. 4 (lower curve). In the range 1.6 – 20 °K, a second set of data represents the variation of the $2s$ excitonic level. They have only been resolved at very low temperature. The temperature dependence of the band gap is obtained from the energy position of the $1s$ peak shifted up by 14.5 meV and is shown as black dots on the upper curve.

In Fig. 5 we show some typical absorption spectra obtained at 293 , 270 , 208 , 135 , 90 , and 1.6 °K. The spectrum at 1.6 °K is shown for comparison. We note the very fast ionization of the excitonic ground state with increasing temperature which supports our rather small binding energy. It appeared interesting to fit all spectra with the theoretical formulation of Sec. III allowing only the broadening parameter to vary. The results are shown as open circles on the experimental spectra (full line) and permit a line-shape determination of the band gap. The overall agreement is very good except for the low absorption levels in Fig. 5. This was already noted at 1.6 °K. A summary of all relevant parameters is given in Table III.

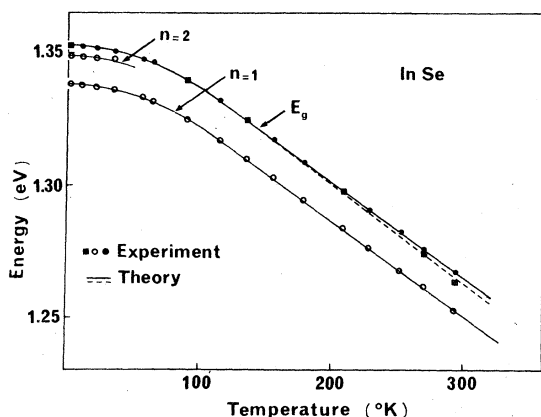


FIG. 4. Temperature dependence of the band-edge and excitonic structures in InSe. The various lines correspond to the theoretical model discussed in the text. \circ energy position of the $1s$ and $2s$ exciton peaks. \bullet energy position of the $1s$ structure shifted up by 14.5 meV. \blacksquare band-gap energies as obtained from the curve-fitting procedure. The theoretical lines are discussed in the text and correspond with $B = 17.2$ meV $^{1/2}$ (broken line) and $B = 16.8$ meV $^{1/2}$ (full line).

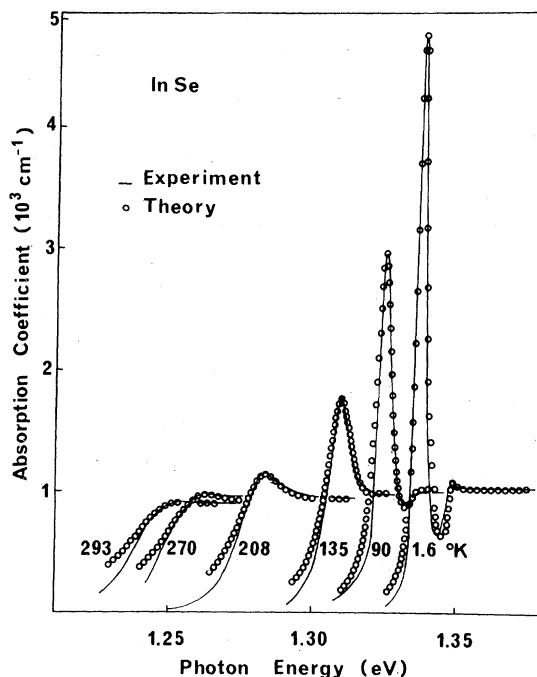


FIG. 5. Typical absorption spectra obtained at 293 , 270 , 208 , 135 , 90 , and 1.6 °K. The theoretical model allows only the broadening parameter to vary as a function of temperature. It reproduces satisfactorily the main features of the spectra.

First note the constant value of A and R_0 which enter the calculation throughout the temperature range. They are not free parameters but characteristic constants of InSe, independent of the temperature. This was already pointed out in Sec. III. Also note the satisfactory agreement between our experimental linewidth and the best value of the broadening parameter which reproduces the strength of the excitonic structure. Finally, note in Fig. 5 that, in agreement with the experimental findings, the calculation reproduces well the decrease in the absorption strength above the band gap when the temperature increases. This is only an effect of lifetime broadening and is not correlated with a change in oscillator strength. The square symbols in Fig. 4 (upper curve) show the different band-gap energies obtained from Table III. At low temperature they are in very good agreement with the position of the excitonic peak shifted up by 14.5 meV. Above 200 °K a systematic discrepancy appears which is about 3 meV at 293 °K. It shows that one underestimates slightly the temperature dependence of the band gap if one neglects the broadening induced shift of the excitonic structure. The discrepancy, however, remains very small: one obtains $dE/dT = 3.6 \times 10^{-4}$ eV/°K from the shift in energy of the $1s$ maximum

TABLE III. Summary of the parameters used in the calculation. Note the constant values of the normalization constant A and the Rydberg energy R_0 . We give the experimental values of the broadening parameter within brackets. The theoretical values have been chosen to match the excitonic absorption strength. Note the good overall agreement.

$T(^{\circ}\text{K})$	1.6	90	135	208	270	293
A (cm^{-1})	1050	1050	1050	1050	1050	1050
R_0 (meV)	14.5	14.5	14.5	14.5	14.5	14.5
Γ (meV)	2.0	3.3	6	9.9	14.9	17.2
(experiment)	(2.0)	(3.3)	(6)	(10)	(14)	(17)
E_g (meV)	1352.5	1339.5	1324.5	1297.5	1274	1263.5

and 3.7×10^{-4} eV/ $^{\circ}\text{K}$ from the shift of the band edge as obtained from the curve-fitting procedure.

B. Discussion

For a given semiconductor, the variation of the band gap versus temperature is dependent on three contributions²⁶: (i) a simple dilatation effect in which the constituting atoms are supposed to move rigidly versus lattice expansion, (ii) a reduction of the ionic potential which corresponds to the mean square displacement of atoms around their equilibrium position (this is the so-called Debye-Waller effect), and (iii) a change in electron-phonon interaction which results in an additional shift (self-energy effect) and necessarily reduces the band gap when the temperature increases. The relative contribution of the different mechanisms to the experimental shift are difficult to weigh. For cubic compounds,²⁷ the variations observed are well accounted for by lattice expansion and Debye-Waller effects only. On the other hand, for GaSe, the experimental results have been mainly correlated with the electron-phonon interaction^{28,29} and lattice expansion effects.²⁹ It should be noted that both GaSe and GaS have a negative pressure coefficient²⁹ ($dE_g/dP \sim -4 \times 10^{-6}$ eV/bar) so the corresponding contribution is positive: the dilatation effect increases the band gap when the temperature increases and partly cancels the self-energy contribution. In the case of GaSe, the resulting variation is well accounted for by one phonon mode only^{28,29} whose energy, ~ 16.5 meV, closely correlates with the lowest A_{1g} optical mode. Taking account of the difference in atomic masses between GaSe and InSe⁷ we have found it interesting to check how a 14-meV phonon does fit the temperature dependence of the band edge for InSe. The result is shown as full and dotted lines in Fig. 4 and compares well with our experimental data.

For layer compounds with a three-dimensional character, the self-energy contribution obeys the equation¹²

$$\Delta E = -B(\hbar\Omega)^{1/2}/(e^{\hbar\Omega/kT} - 1), \quad (4)$$

where $\hbar\Omega$ is the phonon energy and B a normalization constant

$$B = (8 \ln 2 / \pi) g^2 (\hbar^2 Q^2 / 2 m^*)^{1/2}. \quad (5)$$

g is a dimensionless electron-phonon coupling constant, m^* the effective mass of carriers, and Q an effective Brillouin-zone radius. In Fig. 4, we must slightly change the normalization constant from 16.8 to 17.2 meV^{1/2} in order to get the best overall agreement with (a) the peak of the $n=1$ exciton shifted up by 14.5 meV (full line), or (b) the band-edge energy directly obtained from the curve-fitting procedure (dotted line). Both results are in fairly good agreement with the experimental data and, within experimental accuracy, support an average value

$$B = 17.0 \pm 0.2 \text{ meV}^{1/2}.$$

They show also that an identical phonon mode of energies 14 and 16.5 meV couple strongly with the charge carriers in InSe and GaSe, respectively. This supports the GaSe-like scheme for InSe.

It is often convenient to approximate the temperature dependence of the band gap with a simple analytical expression. From Eqs. (4) and (5), with $B = 17 \text{ meV}^{1/2}$, we obtain

$$E_T(\text{meV}) = 1352.5 - 65/(e^{162/T} - 1), \quad (6)$$

where T is the sample temperature in degrees Kelvin and E_T the band-gap energy in meV. In the full temperature range ($0 < T < 300$ K), this expression is accurate within 1 meV.

The last point we want to investigate is the temperature dependence of the excitonic lifetime (broadening parameter) versus temperature. With the same short-range, three-dimensional, electron-optical phonon interaction dominating the excitonic lifetime, the two processes associated with the emission and absorption, respectively, of a 14-meV phonon obey the equations

$$\tau_e^{-1} = (2/\hbar) g^2 (n+1) [\hbar\Omega(\epsilon - \hbar\Omega)]^{1/2} \quad (\text{emission}), \quad (7)$$

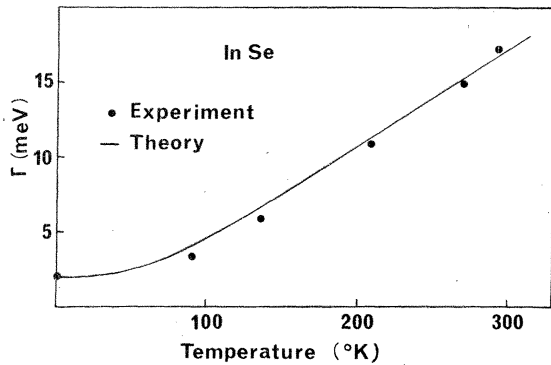


FIG. 6. Change in broadening parameter (exciton lifetime) versus temperature. The theoretical model (full line) corresponds to a short-range, three dimensional, electron-phonon interaction discussed in the text.

$$\tau_a^{-1} = (2/\hbar)g^2n[\hbar\Omega(\epsilon + \hbar\Omega)]^{1/2} \quad (\text{absorption}), \quad (8)$$

where ϵ is the kinetic energy associated with the k extension of excitonic wave functions (typically it should be around 1 effective Ry).

Combining Eqs. (7) and (8) with $\Gamma = \hbar/2\tau$, we get

$$\tau(T) = \Gamma_0(1 + \alpha n), \quad (9)$$

where n is the phonon occupation number, $\alpha = [(\epsilon + \hbar\Omega)^{1/2}/(\epsilon - \hbar\Omega)]$, and $\Gamma_0 = g[\hbar\Omega(\epsilon - \hbar\Omega)]^{1/2}$. The lower the energy difference ($\epsilon - \hbar\Omega$), the lower the asymptotic limit at 0°K (Γ_0) and the stronger the temperature dependence of the band gap. This can be viewed as an example of resonance in electron-phonon interaction.

With the phonon energy $\hbar\Omega = 14$ meV, the best fit

in Fig. 6 is obtained with $\epsilon = 15$ meV in very good agreement with our previous estimate from the determination of the effective Rydberg energy. Finally, from the low-temperature limit $\Gamma_0 = 2$ meV, we get $g \approx 0.5$, which constitutes the first estimate of the electron-phonon coupling constant in InSe. The value obtained is in very good agreement with two recent results published independently for GaSe.^{23,28}

IV. CONCLUSION

We have investigated the direct absorption edge of InSe. Three components of the excitonic series have been resolved for the first time and we have obtained a new and accurate value for the Rydberg energy, $R_0 = 14.5$ meV. From this value an effective mass $m_e = 0.10 m_0$ for electrons in the Γ minimum of the conduction band has been obtained. We have also analyzed the absorption spectrum with a three-dimensional model and found a very good agreement. From the analysis an interband matrix element $P_{\perp}^2 = 0.6$ eV has been deduced. Next we have investigated the temperature dependence of the fundamental edge. We have found a strong interaction with a 14-meV phonon which accounts for (i) the shift of the band-gap energy and (ii) the change in broadening parameter. A simple power law has been found which describes the temperature dependence of the band gap. Finally, we have estimated the electron-phonon coupling constant; we find $g \sim 0.5$.

ACKNOWLEDGMENTS

We thank Dr. Bastide for constant help with the computational part of the work.

*Laboratoire associé au CNRS.

¹For a general review of the recent work on layer compounds, see Nuovo Cimento B 38, 153 (1977).

²G. Ottavia, C. Canali, F. Nava, P. Schmid, E. Mooser, R. Minder, and I. Zschokke, Solid State Commun. 14, 933 (1974).

³A. Likhforman, D. Carre, J. Etienne, and B. Bachet, Acta Crystallogr. B 31, 1252 (1975).

⁴M. K. Andriyashik, M. Yu. Sakhnovskii, V. B. Timofeev, and A. S. Yakimova, Phys. Status Solidi 28, 2776 (1968). See also M. Yu Sakhnovskii, V. B. Timofeev, and A. S. Yakimova, Sov. Phys.-Semicond. 2, 168 (1968).

⁵V. V. Sovolev, and V. I. Donetskiikh, Inorg. Mater. 8, 1229 (1972).

⁶R. H. Williams, J. V. McCanny, R. B. Murray, L. Ley, and P. C. Kemeny, J. Phys. C 10, 1223 (1977).

⁷A. Segura, J. M. Besson, A. Chevy, and M. S. Martin, Nuovo Cimento B 38, 345 (1977).

⁸A. Mercier and J. P. Voitchovsky, Phys. Rev. B 11, 2243 (1975).

⁹J. V. McCanny and R. B. Murray, J. Phys. C 10, 1211 (1977).

¹⁰R. J. Elliott, Phys. Rev. 108, 1384 (1957).

¹¹D. D. Sell and P. Lawaetz, Phys. Rev. Lett. 26, 311 (1971).

¹²Ph. Schmid, Nuovo Cimento B 21, 258 (1974). See also R. C. Fivaz and Ph. Schmid in *Electrical and Optical Properties*, edited by P. A. Lee (Reidel, Boston, 1976), p. 343.

¹³A. Chevy, A. Kuhn, and M. S. Martin, J. Cryst. Growth 38, 118 (1977).

¹⁴J. Pascual, J. Camassel, and H. Mathieu, Phys. Rev. B (to be published).

¹⁵B. Celustka, A. Persin, and D. Bidjin, J. Appl. Phys. 41, 813 (1970).

¹⁶M. Schlüter, Nuovo Cimento B 13, 313 (1973).

¹⁷M. Schlüter, J. Camassel, S. Kohn, J. P. Voitchovsky, Y. R. Shen, and M. L. Cohen, Phys. Rev. B 13, 3534 (1976).

¹⁸E. Avlich, J. L. Brebner, and E. Mosser, Phys. Status Solidi 31, 129 (1969).

- ¹⁹Y. Depeursinge, *Nuovo Cimento B* 38, 153 (1977).
- ²⁰J. M. Besson, R. Le Toullec, and N. Piccioli, *Phys. Rev. Lett.* 39, 671 (1977).
- ²¹M. Grandolfo, E. Gratton, F. Anfosso Soma, and P. Vecchia, *Phys. Status Solidi B* 48, 729 (1971).
- ²²A. Balzarotti and M. Piacentini, *Solid State Commun.* 10, 421 (1972).
- ²³C. Manfredotti, A. M. Mancini, R. Murri, A. Rizzo, and L. Vasenelli, *Nuovo Cimento B* 39, 257 (1977).
- ²⁴C. Manfredotti, R. Murri, A. Rizzo, L. Vasanelli, and G. Micocci, *Phys. Status Solidi A* 29, 475 (1975).
- ²⁵C. Hermann and C. Weisbuch, *Phys. Rev. B* 15, 823 (1977).
- ²⁶G. Harbeke and E. Tosatti, *Proceedings of the International Conference on the Physics of Semiconductors, Stuttgart, 1974*, edited by M. H. Pilkuh (Teubner, Stuttgart, 1974), p. 626.
- ²⁷J. Camassel and D. Auvergne, *Phys. Rev. B* 12, 3258 (1975).
- ²⁸Ph. Schmid and J. P. Voitchovsky, *Phys. Status Solidi B* 65, 249 (1974).
- ²⁹J. M. Besson, *Nuovo Cimento B* 38, 478 (1977).